Eco. Env. & Cons. 31 (April Suppl. Issue) : 2025; pp. (S101-S109)
Copyright@ EM International
ISSN 0971–765X

DOI.: http://doi.org/10.53550/EEC.2025.v31i03s.018

Flood Susceptibility Mapping of Lakhimpur District of Assam using GIS-Based Multi-Criteria Decision Analysis

Shyamal Borah* and Karishma Sarma

Department of Geography, Cotton University, Guwahati, Assam, India

(Received 18 October, 2024; Accepted 4 January, 2025)

ABSTRACT

This study assesses flood susceptibility in Lakhimpur district, Assam, India, using a GIS-based multi-parametric approach and Analytical Hierarchy Process (AHP). Analyzing 10 flood conditioning factors, the study reveals 45.20% (1029.20 sq. km) of the district is highly susceptible, 52.86% (1203.62 sq. km) moderately susceptible, and 2% (45.50 sq. km) low susceptible. The district's alluvial plains, heavy monsoon rainfall, and significant river discharge contribute to its high flood vulnerability. The resulting flood susceptibility map serves as a critical tool for local authorities and stakeholders to develop and implement effective flood mitigation strategies, ultimately reducing damage and loss of life in this flood-prone region.

Key words: *Flood Susceptibility, GIS, Analytical Hierarchy Process (AHP), Multi-parametric Analysis*

Introduction

Floods are among the most devastating natural disasters, particularly in low-income countries, causing significant damage to property and loss of life (Rentschler *et al.*, 2022). According to Rentschler et al., 2022, more than 1.81 billion people, or 23% of the world's population, are directly exposed to 1-in-100-year floods, with India accounting for over one-third of this exposure, affecting approximately 390 million people. Additionally, about 40 million hectares of land, roughly one-eighth of India's geographical area, are prone to floods (Singh and Kumar, 2013). Floods in India predominantly occur due to the extreme spatial and temporal variations in the rainfall pattern over the short monsoon period of 3-4 months, resulting in heavy river discharge. The Ganga and Brahmaputra basins are among India's most chronic flood-prone areas. Over the past thirty years, India has experienced significant floods, including those in Bihar (1987, 2004, 2008), Uttarakhand (2013), Jammu & Kashmir (2014), Ladakh (2010), Assam (1998, 2012), Maharashtra (2005), and Chennai (2015) (Nandargi & Shelar, 2018). Lakhimpur, a district in Assam, is particularly vulnerable to flooding due to its topography, climate, and hydrological features (Figure 1). Situated in the Brahmaputra river basin, it is characterized by a subtropical and humid climate with an annual average rainfall of 2949.6 mm, receiving maximum rainfall during the monsoon season. The district experiences Southwest monsoon rainfall from April to September/October, with the highest rainfall areas located near the foothills of the Arunachal Himalayas in the northern part of the district. The River Subansiri and its tributaries, originating from the Eastern Himalayas, exacerbate flooding in Lakhimpur during the monsoon period due to heavy and continuous rain spells lasting several days. This study aims to study the flood susceptibil-

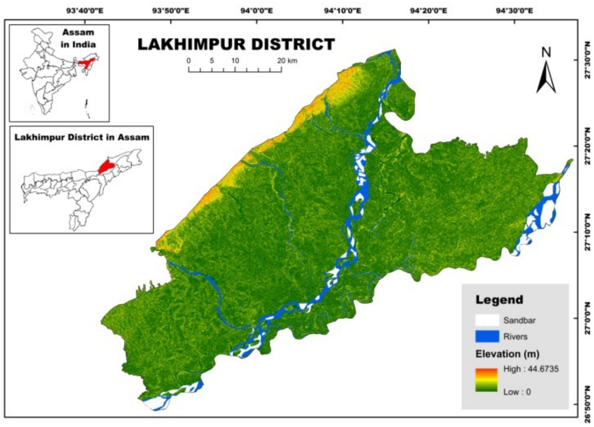

Fig. 1. Map of the study area

ity of the Lakhimpur district using a GIS-based multi-parametric approach. By identifying areas at high risk of flooding, this research seeks to provide valuable insights for local authorities and stakeholders in planning and implementing effective flood management strategies.

Database and Methodology

This study utilized various data sources, including satellite images, digital elevation models (DEM), rainfall data, soil data, and road network data (Table 1). The methodology for assessing flood susceptibility in the Lakhimpur district involves a systematic approach, integrating Geographic Information System (GIS) techniques and the Analytical Hierarchy Process (AHP). This approach ensures a comprehensive analysis of various flood conditioning factors, providing robust insights into flood risk areas. All spatial data were pre-processed and georeferenced to the WGS_84 datum and UTM Zone 46N coordinate system to ensure uniformity and accuracy in spatial analysis. The data sources utilized in this study include satellite images, digital elevation models (DEM), rainfall data, soil data, and road network data. Satellite images, specifically Landsat 8 OLI images, were used to extract land use and land cover (LULC) information, while DEM data from the Shuttle Radar Topography Mission (SRTM) provided detailed elevation and slope information.

This flood susceptibility analysis utilized ten relevant factors, categorized into four groups: topographical (elevation, slope, and topographic wetness index), climatic (rainfall deviation), hydrographical (distance from river and drainage density), and local (land use and land cover, soil type, normalized difference vegetation index, and road network). Thematic maps were prepared using various data sources, including Digital Elevation Model (DEM) for topographical factors, Landsat OLI images for land use and land cover, NDVI, and distance from river, climatic data for rainfall, road network data, and soil data. The methodology involved data reclassification, Analytical Hierarchy Process (AHP) modeling, pair-wise index calculation, weight assignment to factors, and overlay analysis. Finally,

Table 1. Details of the dataset used

Sl. No	Flood conditioning factors	Details	Data type
1	Elevation	Shuttle Radar Topography Mission Digital Elevation Model (SRTM DEM), 2014(https:// earthexplorer.usgs.gov)	Raster, 30 m
2	Slope	Shuttle Radar Topography Mission Digital Elevation Model (SRTM DEM), 2014(https:// earthexplorer.usgs.gov)	Raster, 30 m
3	Topographic wetness index	Shuttle Radar Topography Mission Digital Elevation Model (SRTM DEM), 2014(https:// earthexplorer.usgs.gov)	Raster, 30 m
4	Land use and land cover	Landsat 8 OLI, December 30th, 2023 (https:// earthexplorer.usgs.gov)	Raster, 30 m
5	Rainfall deviation	Average rainfall during 2022-2023, CRU	Vector (point)
6	Distance from river	Landsat 8 OLI, December 30th, 2023 (https:// earthexplorer.usgs.gov)	Vector (polyline)
7	Normalized difference vegetation index	Landsat 8 OLI, December 30th, 2023 (https:// earthexplorer.usgs.gov)	Raster, 30 m
8	Drainage density	Shuttle Radar Topography Mission Digital Elevation Model (SRTM DEM), 2014(https:// earthexplorer.usgs.gov)	Raster, 30 m
9	Soil type	Food and Agriculture Organization of the United Nations	Vector (point)
10	Distance from road	BBBike extracts open street map	Vector (polyline)

Source: Authors

the flood susceptibility map was generated using ArcGIS 10.8 software, as outlined in Figure 2.

Flood conditioning factors

Elevation (E): Elevation of a region is a dominating factor for flood occurrence. Water tends to flow from elevated regions to flat regions. Regions with high elevations are less prone to flood as compared to flat areas (Ramesh and Iqbal, 2022). Topographical factors, which are affected directly by the extent of flow and runoff speed, play a significant role in the occurrence of floods in an area.

Slope (S): Slope plays an important role in flood occurrence in a region. The slope of any area directly impacts the surface runoff, velocity of water flow and soil erosion and thus is considered a major factor in the occurrence of flood and controls the vertical infiltration of water (Ribolzi *et al.*, 2011).

Topographic wetness index (TWI): The spatial wetness distribution is the topographic wetness index (TWI), which controls the over land water flow of an area. TWI has an important impact on flood zoning. TWI was calculated based on the equation proposed by (Beven and Kirkby, 1979).

TWI = ln (flow accumulation)/ (tan slope)

Land use land cover (LULC): Land use and land cover have a vital role in determining the flood of an area as it governs various hydrological processes such as runoff generation, infiltration and evapotranspiration. The types of land use significantly control runoff and flood potential (Wheater and Evans, 2009). Areas with high vegetation cover are at low risk.

Rainfall deviation (RF): A high-intensity rainfall event can overwhelm the capacity of drainage systems and can cause a flash flood in a short period of time (SOURCE). Rainfall mainly occurs during the summer monsoon season, which causes flood disasters in Assam. In our study, the deviation of rainfall was considered as a factor for flood susceptibility analysis as positive deviation gives a clear indication of flood possibility. The inverse distance weighting (IDW) interpolation method (Ullah and Zhang, 2020) was used to prepare a rainfall deviation map in ArcGIS 10.8 and grouped into five classes using the natural break interval tool.

Distance from rivers (DR): Areas situated near a river are at a greater risk of flooding as compared to far-located ones, and thus, the distance from the river is one of the important factors considered for the study. River banks and nearby low-lying flood-

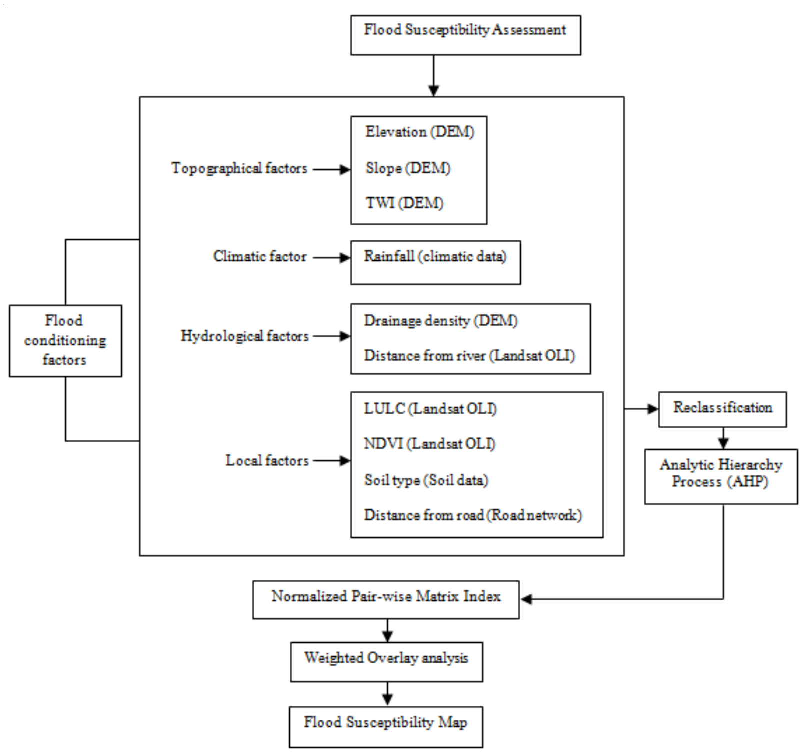

Fig. 2. Methodological flow chart of the study

plains are highly affected by floods (Samanta *et al.*, 2018).

Normalized difference vegetation index (NDVI): The NDVI is an important index to assess the vegetation cover of an area that ranges between -1 and + 1, which has a significant impact on the intensity of flood in a basin. Hence, NDVI of the Lakhimpur district was taken as another variable that was developed based on the formula given below (Khosravi *et al*., 2016).

NDVI = (NIR – VIR) / (NIR + VIR)

Where NIR = near-infrared band

VIR = Visible infrared band

Drainage density (DD): The drainage density is also a major factor that strongly contributes to flood in a region. Runoff in a basin is directly affected by the drainage density per unit area. Regions with high river density are more prone to flood risk (Zhang *et al.,* 2020). Here, the density of drainage was evaluated using ArcGIS 10.8.

Distance from road (RD): Distance from road also impacts the flood occurrence in any region. The concrete roads facilitate easy flow of runoff that may contribute in flood incidence. However, the accumulation of water at ditches and pools along the roads attenuates the runoff intensity, but such ditches are not permanent factors as they are renovated from time to time.

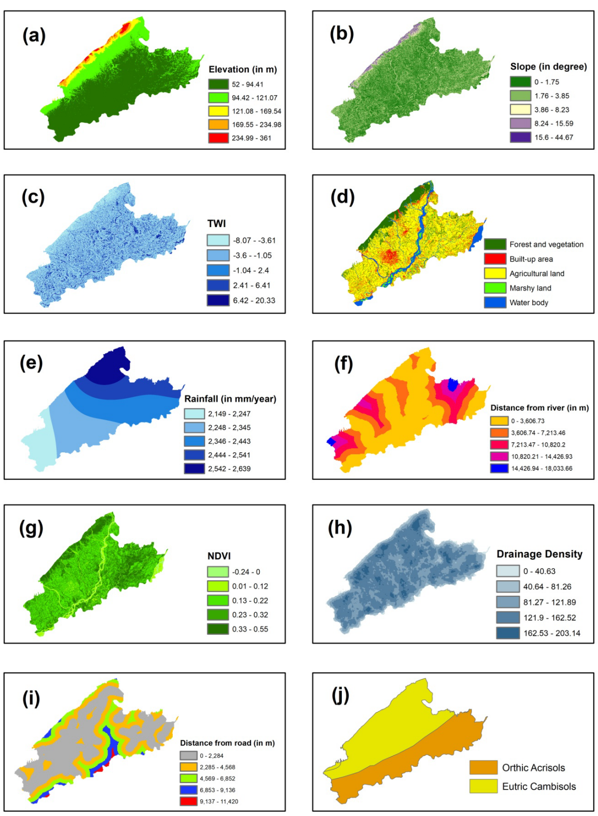

Fig. 3. Flood conditioning factors: (a) elevation, (b) slope, (c) TWI, (d) LULC, (e) Rainfall, (f) Distance from river, (g) NDVI, (h) drainage density, (i) Distance from road, (j) soil type.

Soil type: The content of clay in soil is also a very important element in flood analysis. Spatial soil map was created using ArcGIS 10.8 with the help of inverse distance weighting interpolation technique.

Analytical hierarchy process and weight combination approach: Analytical hierarchy process is a decision-making approach which is designed based on hierarchical structure for decision making (Saaty, 2008). The Analytical Hierarchy Process (AHP) utilizes the Weight Combination Approach (WCA) for multi-parametric decision-making, determining the relative significance of paired criteria to achieve a set goal. AHP involves hierarchical problem formulation, prioritization, and paired comparisons to assess element importance. This simple, flexible method provides precise results, making it ideal for flood susceptibility mapping. AHP quantitatively evaluates alternatives, incorporating subjectivity and expertise through Saaty's verbal scale (Table 2). Rank values (1-9) are assigned to controlling factors based on relative importance. A pair-wise comparison matrix is then prepared to evaluate flood-inducing factors, despite AHP's limitations of extensive computations and time-consuming processes. Weight values of each flood conditioning factor were calculated and consistency ratio (CR) was calculated (Vaidya and Kumar, 2006). The Random Consistency Index (RCI) represents the mean CI values of various comparison matrices, as outlined by Saaty (2008) in Table 3. For this study, involving 10 flood conditioning factors, the corresponding RCI value is 1.49, serving as a reference to evaluate the consistency of the pair-wise comparison matrix.

Consistency ratio = CI/RI

Table 2. Defined scale to compare two flood conditioning factors

Intensity of importance	Meaning
1	Equal importance
3	Moderate importance
5	Strong importance
7	Very strong importance
9	Extreme importance

Table 3. Random consistency index

n (matrix value)	1	2	3	4	5	6	7	8	9	10
RI	0	0	0.58	0.90	1.12	1.24	1.32	1.41	1.45	1.49

Source: (Saaty, 2008)

Where,

CI (consistency index) = $(\lambda\text{-n})/(\text{n-1})$

N is the number of factors, and λ is the average value of the consistency vector

RI = Random index (1.49 for 10 parameters)

Results

The flood susceptibility map of Lakhimpur district reveals varied flood risk levels, derived from analyzing 10 factors (Figure 3). Elevation ranges from 52m-361m, with highest levels in the north and lowest in central and southern areas. Slope varies from 0°-44.67°, while Topographic Wetness Index (TWI) is grouped into five classes. Land use/land cover classification includes agricultural land (45.78% dominant), built-up areas, forest, marshy land, and water bodies. Rainfall distribution increases from southwest to north (2149-2639 mm/year), with proximity to rivers, NDVI (-0.24 to 0.55), drainage density (0-203.14 m/km), and road network distance (five classes) also influencing flood risk, as detailed in Figures 3 and Tables 4.

Pair-wise (Table 5) and normalized pair-wise (Table 6) comparison matrices using AHP resulted in a consistency ratio (CR) of -0.67 (Table 7), acceptable for decision-making as it falls within the 0 to 0.1 range. The final weights assigned to each factor based on geographical characteristics, background knowledge, and prior studies (Liuzzo *et al.,* 2019), are shown in Table 4.

Lakhimpur district's flood susceptibility was assessed using 10 images with 30m resolution, categorizing the area into three zones: low, moderate, and high susceptibility (Table 8, Figure 4). Results show 45.20% (1029.20 sq. km) is highly susceptible, 52.86% (1203.62 sq. km) moderately susceptible, and 2% (45.50 sq. km) has low susceptibility. High susceptibility zones, primarily in the southern district, are characterized by low elevation, proximity to rivers, gentle slopes, and high drainage density, exacerbated by the Subansiri River and its tributaries' confluence, indicating increased flood probability.

Discussion

Although the results and the spatial flood suscepti-

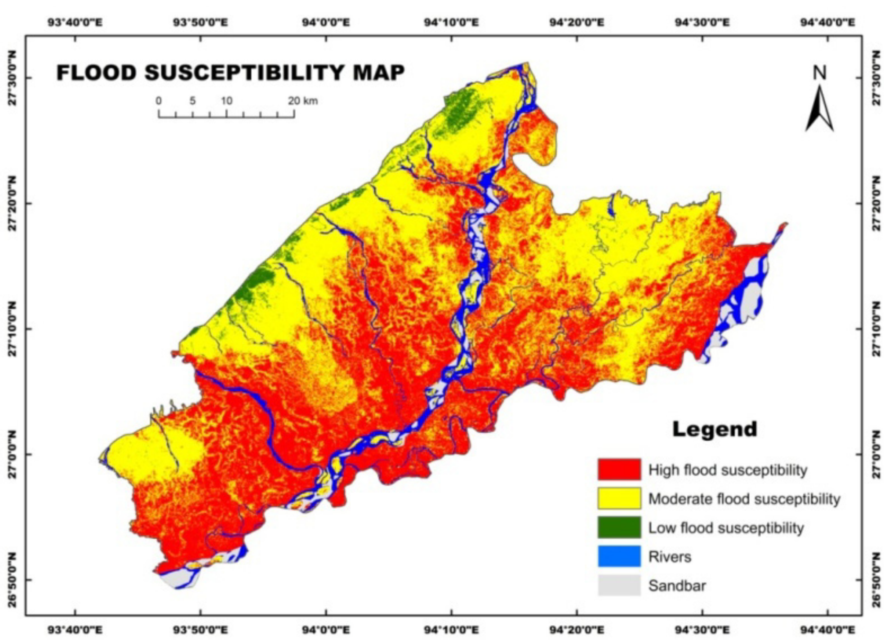

Fig. 4. Flood susceptibility map of Lakhimpur District

Table 4 Classes of flood conditioning factors and weight

Flood causative criteria	Unit	Class	Rank (very high = 5, very low = 1)	Category/intensity	Weight (%)
Elevation	M	52 – 94.41	5	Very high	13
		94.42 – 121.07	4	High	
		121.08 – 169.54	3	Moderate	
		169.55 – 234.98	2	Low	
		234.99 - 361	1	Very low	
Slope	Degree	0 – 1.75	5	Very high	12
		1.76 – 3.85	4	High	
		3.86 – 8.23	3	Moderate	
		8.24 – 15.59	2	Low	
		15.6 – 44.67	1	Very low	
Drainage Density	m/km	0 – 40.63	1	Very low	8
		40.64 – 81.26	2	Low	
		81.27 – 121.89	3	Moderate	
		121.9 – 162.52	4	High	
		162.53 – 203.14	5	Very high	
Distance from river	M	0 – 3606.73	5	Very high	13
		3606.74 – 7213.46	4	High	
		7213.47 – 10820.2	3	Moderate	
		10820.21 – 14426.93	2	Low	
		14426.94 – 18033.66	1	Very low	
TWI	Level	-8.07 to -3.61	1	Very low	4
		-3.6 to -1.05	2	Low	
		-1.04 – 2.4	3	Moderate	
		2.41 – 6.41	4	High	
		6.42 – 20.33	5	Very high	
Rainfall	mm/year	2149 – 2247	1	Very low	5
		2248 – 2345	2	Low	
		2346 – 2443	3	Moderate	
		2444 – 2541	4	High	
		2542 – 2639	5	Very high	
NDVI	Level	-0.24 – 0	5	Very high	13
		0.01 – 0.12	4	High	
		0.13 – 0.22	3	Moderate	
		0.23 – 0.32	2	Low	
		0.33 – 0.55	1	Very low	
Soil type	Level	Orthic Acrisols	3	Moderate	12
		Eutric Cambisols	2	low	
Distance from road	M	0 – 2284	5	Very high	4
		2285 – 4568	4	High	
		4569 – 6852	3	Moderate	
		6853 – 9136	2	Low	
		9137 - 11420	1	Very low	
LULC	Class	Agricultural land	3	Moderate	16
		Built-up area	2	Low	
		Forest and vegetation	1	Very low	
		Marshy land	4	High	
		Water body	5	Very high	

Source: Authors

Table 5. Pair-wise comparison matrix

Factors	E	S	DD	D River	TWI	R	NDVI	ST	D Road	LULC
E	1	1	2	2	3	3	1	1	2	1
S	1	1	2	1	2	3	1	1	2	1
DD	1	0.5	1	0.2	3	3	0.5	1	3	0.33
D River	1	1	5	1	5	3	0.5	1	3	0.5
TWI	1	0.5	0.33	0.2	1	1	0.5	0.2	1	0.33
R	1	0.33	0.33	0.3	1	1	0.33	0.33	3	0.5
NDVI	1	1	2	2	2	3	1	2	3	0.5
ST	1	1	1	1	5	3	0.5	1	5	0.5
D Road	1	0.5	0.33	0.3	1	0.33	0.33	0.2	1	0.33
LULC	1	1	3	2	3	2	2	2	3	1
Total	10	7.83	17	10	26	22.33	7.66	9.73	26	6

Source: Authors

Table 6. Normalized pair-wise comparison matrix

Factors	E	S	DD	D River	TWI	R	NDVI	ST	D Road	LULC	Total	Criteria Weight
E	0.1	0.127	0.117	0.2	0.115	0.134	0.130	0.102	0.076	0.166	1.271	0.127
S	0.1	0.127	0.117	0.1	0.076	0.134	0.130	0.102	0.076	0.166	1.133	0.113
DD	0.1	0.063	0.058	0.02	0.115	0.134	0.065	0.102	0.115	0.055	0.831	0.083
D River	0.1	0.127	0.294	0.1	0.192	0.134	0.065	0.102	0.115	0.083	1.315	0.131
TWI	0.1	0.063	0.019	0.02	0.038	0.044	0.065	0.020	0.038	0.055	0.466	0.046
R	0.1	0.042	0.019	0.03	0.038	0.044	0.043	0.034	0.115	0.083	0.551	0.055
NDVI	0.1	0.127	0.117	0.2	0.076	0.134	0.130	0.205	0.115	0.083	1.291	0.129
ST	0.1	0.127	0.058	0.1	0.192	0.134	0.065	0.102	0.192	0.083	1.156	0.115
D Road	0.1	0.063	0.019	0.03	0.038	0.014	0.043	0.020	0.038	0.055	0.424	0.042
LULC	0.1	0.127	0.176	0.2	0.115	0.089	0.260	0.205	0.115	0.166	1.557	0.155

Source: Authors

Table 7. Calculation of CR

Factors	E	S	DD	D River	TWI	R	NDVI	ST	D Road	LULC	Weighted Sum Value	Ratio
E	0.01	0.01	0.009	0.02	0.005	0.007	0.01	0.01	0.003	0.02	0.13	1.05
S	0.01	0.01	0.009	0.01	0.003	0.007	0.01	0.01	0.003	0.02	0.11	1.05
DD	0.01	0.007	0.004	0.002	0.005	0.007	0.008	0.01	0.004	0.008	0.07	0.89
D River	0.01	0.01	0.02	0.01	0.008	0.007	0.008	0.01	0.004	0.01	0.11	0.90
TWI	0.01	0.007	0.001	0.002	0.001	0.002	0.008	0.002	0.001	0.008	0.04	1.06
R	0.01	0.004	0.001	0.003	0.001	0.002	0.005	0.003	0.004	0.01	0.05	0.99
NDVI	0.01	0.01	0.009	0.02	0.003	0.007	0.01	0.02	0.004	0.01	0.13	0.89
ST	0.01	0.01	0.004	0.01	0.008	0.007	0.008	0.01	0.008	0.01	0.10	0.89
D Road	0.01	0.007	0.001	0.003	0.001	0.0008	0.005	0.002	0.001	0.008	0.04	1.09
LULC	0.01	0.01	0.014	0.02	0.005	0.004	0.03	0.02	0.004	0.02	0.16	1.07
Total												9.88
	Ë max = 9.88/10= 0.988				CI = 0.988-10/10-1= -1					CR = -1/1.49= -0.67		

Source: Authors

Table 8. Statistics of flood susceptibility classes of Lakhimpur District

Sl. No.	Susceptibility class	FSI	Area (km^2)	Area (%)
1	High	4	1029.20	45.20
2	Moderate	3	1203.62	52.86
3	Low	2	45.50	2

Source: Authors

bility map of the Lakhimpur district proposed in our study will be very useful for flood management, the study has some limitations, too. Firstly, the number of flood-causing factors to be considered is the major drawback in terms of flood susceptibility analysis, as there is no guideline specifying the selection of controlling factors. Although we have selected ten flood conditioning factors, researchers have considered four to twelve factors which suggests that there is no general agreement on the factors (Choubin *et al.*, 2019). This study's AHP-based flood susceptibility analysis has limitations, including potential errors in weight assignment due to data availability and researcher expertise. Additionally, variations in data format, scale, and generalization may affect results. Future research will focus on addressing data consolidation and integration challenges, exploring alternative models, and comparing spatial maps to identify suitable alternatives and improve flood susceptibility assessments.

The flood susceptibility map produced in this study has numerous practical applications, enhancing flood management and mitigation efforts in Lakhimpur district. It informs urban planning, infrastructure development, environmental conservation, agricultural planning, emergency management, and insurance risk assessment by identifying safe zones for development, guiding flood-resilient infrastructure design, protecting ecologically sensitive zones, and supporting informed agricultural planning and emergency preparedness, ultimately contributing to a more resilient and flood-prepared district.

Conclusion

This study provides a comprehensive flood susceptibility map for Lakhimpur district using a GIS-based multi-parametric approach with AHP. The findings highlight the critical areas at risk of flooding, which can aid in effective flood management and planning. The integration of various flood conditioning factors ensures a robust analysis, offering valuable insights for policymakers. Future research should focus on incorporating real-time flood monitoring and prediction systems to enhance the region's flood resilience. Implementing structural and non-structural flood mitigation measures based on the identified high-risk areas is crucial for minimizing flood impacts.

Statements and Declarations

Conflict of interest: The corresponding author declares on behalf of all authors that there is no conflict of interest.

Funding: There was no fund provided for the research work.

References

Beven, K.J. and Kirkby, M.J. 1979. A physically based, variable contributing area model of basin hydrology / Un modèle à base physique de zone d'appel variable de l'hydrologie du bassin versant. *Hydrological Sciences Bulletin.* 24(1): 43-69. https://doi.org/10.1080/02626667909491834

Choubin, B., Moradi, E., Golshan, M., Adamowski, J., Sajedi-Hosseini, F. and Mosavi, A. 2019. An ensemble prediction of flood susceptibility using multivariate discriminant analysis, classification and regression trees, and support vector machines. *Science of The Total Environment*. 651: 2087-2096. https://doi.org/10.1016/j.scitotenv.2018.10.064

Khosravi, K., Nohani, E., Maroufinia, E. and Pourghasemi, H.R. 2016. A GIS-based flood susceptibility assessment and its mapping in Iran: a comparison between frequency ratio and weights-of-evidence bivariate statistical models with multi-criteria decision-making technique. *Natural Hazards*. 83(2): 947-987. https://doi.org/10.1007/s11069-016-2357-2

Liuzzo, L., Sammartano, V. and Freni, G. 2019. Comparison between Different Distributed Methods for Flood Susceptibility Mapping. *Water Resources Management.* 33(9): 3155-3173. https://doi.org/10.1007/s11269-019-02293-w

Nandargi, S.S. and Shelar, A. 2018. Rainfall and Flood Studies of the Ganga River Basin in India. *Annals of Geographical Studies.* 1(1): 34-50. https://doi.org/10.22259/2642-9136.0101004

Ramesh, V. and Iqbal, S.S. 2022. Urban flood susceptibility zonation mapping using evidential belief function, frequency ratio and fuzzy gamma operator models in GIS: a case study of Greater Mumbai, Maharashtra, India. *Geocarto International.* 37(2): 581-606. https://doi.org/10.1080/10106049.2020.1730448

Rentschler, J., Salhab, M. and Jafino, B.A. 2022. Flood exposure and poverty in 188 countries. *Nature Communications*. 13(1): 3527. https://doi.org/10.1038/s41467-022-30727-4

Ribolzi, O., Patin, J., Bresson, L.M., Latsachack, K.O., Mouche, E., Sengtaheuanghoung, O., Silvera, N., Thiébaux, J.P. and Valentin, C. 2011. Impact of slope gradient on soil surface features and infiltration on steep slopes in northern Laos. *Geomorphology*. 127(1-2): 53-63. https://doi.org/10.1016/j.geomorph.2010.12.004

Saaty, T.L. 2008. Decision making with the analytic hierarchy process. *International Journal of Services Sciences*. 1(1): 83. https://doi.org/10.1504/IJSSCI.2008.017590

Samanta, D., Hameed, S.N., Jin, D., Thilakan, V., Ganai, M., Rao, S.A. and Deshpande, M. 2018. Impact of a Narrow Coastal Bay of Bengal Sea Surface Temperature Front on an Indian Summer Monsoon Simulation. *Scientific Reports*. 8(1): 17694. https://doi.org/10.1038/s41598-018-35735-3

Singh, O. and Kumar, M. 2013. Flood events, fatalities and damages in India from 1978 to 2006. *Natural Hazards*. 69(3): 1815-1834. https://doi.org/10.1007/s11069-013-0781-0

Ullah, K. and Zhang, J. 2020. GIS-based flood hazard mapping using relative frequency ratio method: A case study of Panjkora River Basin, eastern Hindu Kush, Pakistan. *Plos One*. 15(3): e0229153. https://doi.org/10.1371/journal.pone.0229153

Vaidya, O.S. and Kumar, S. 2006. Analytic hierarchy process: An overview of applications. *European Journal of Operational Research*. 169(1): 1-29. https://doi.org/10.1016/j.ejor.2004.04.028

Wheater, H. and Evans, E. 2009. Land use, water management and future flood risk. *Land Use Policy*. 26: S251-S264. https://doi.org/10.1016/j.landusepol.2009.08.019

Zhang, D., Shi, X., Xu, H., Jing, Q., Pan, X., Liu, T., Wang, H. and Hou, H. 2020. A GIS-based spatial multi-index model for flood risk assessment in the Yangtze River Basin, China. *Environmental Impact Assessment Review*. 83: 106397. https://doi.org/10.1016/j.eiar.2020.106397